NASA MEMO 4-6-59E

NASA

MEMORANDUM

INVESTIGATION OF A 4.5-INCH-MEAN-DIAMETER

TWO-STAGE AXIAL-FLOW TURBINE SUITABLE

FOR AUXILIARY POWER DRIVES

By Robert Y. Wong and Daniel E. Monroe

Lewis Research Center
Cleveland, Ohio

NATIONAL AERONAUTICS AND SPACE ADMINISTRATION

WASHINGTON
March 1959

NATIONAL AERONAUTICS AND SPACE ADMINISTRATION

MEMORANDUM 4-6-59E

INVESTIGATION OF A 4.5-INCH-MEAN-DIAMETER TWO-STAGE AXIAL-FLOW TURBINE SUITABLE FOR AUXILIARY POWER DRIVES

By Robert Y. Wong and Daniel E. Monroe

SUMMARY

The design and experimental investigation of a 4.5-inch-mean-diameter two-stage turbine are presented herein and used to study the effect of size on the efficiency of turbines in the auxiliary power drive class. The results of the experimental investigation indicated that design specific work was obtained at design speed at a total-to-static efficiency of 0.639. At design pressure ratio, design static-pressure distribution through the turbine was obtained with an equivalent specific work output of 33.2 Btu per pound and an efficiency of 0.656.

It was found that, in the design of turbines in the auxiliary power drive class, Reynolds number plays an important part in the selection of the design efficiency. Comparison with theoretical efficiencies based on a loss coefficient and velocity diagrams are presented. Close agreement was obtained between theory and experiment when the loss coefficient was adjusted for changes in Reynolds number to the -1/5 power.

INTRODUCTION

Turbines for driving auxiliary equipment on rocket and space vehicles have become of interest because of the premium placed on space and weight on these vehicles. In general, these turbines are small in size because of the low horsepower requirements of such equipment. In order to minimize the gross weight of the drive system, it is necessary to extract maximum work from each pound of fuel expended. This means that the turbine must be designed for high specific work output and low weight flows, and reasonable efficiencies must be attainable.

Since there is little published information on the performance of turbines in this size class, the NASA is therefore engaged in a program

to study the effect of size on the efficiency of turbines in the auxiliary drive class. As part of this program, a 4.5-inch-mean-diameter two-stage turbine was designed and experimentally investigated. This report presents the design and the results of the experimental investigation. An analysis of the results is also presented to indicate the effect of Reynolds number on efficiency.

SYMBOLS

A	area, sq ft
C	loss coefficient (equal to $K\left(\frac{A}{w}\right)$ in ref. 5)
D_p	pressure-surface diffusion parameter, $1 - \frac{W_{p,min}}{W_i}$
D_s	suction-surface diffusion parameter, $1 - \frac{W_o}{W_{s,max}}$
E_{act}	actual kinetic energy
g	gravitational constant, 32.17 ft/sec^2
$\Delta h'$	specific work output, Btu/lb
hp	horsepower
J	mechanical equivalent of heat, 778 ft-lb/Btu
o	throat dimension, ft
p	absolute pressure, lb/sq ft
R	gas constant, 53.35 ft-lb/(lb)($^\circ$R)
Re	Reynolds number
r	radius, in.
s	blade spacing
T	temperature, $^\circ$R
t	trailing-edge thickness in tangential direction, ft
U	blade velocity, ft/sec
V	absolute gas velocity, ft/sec

W relative gas velocity, ft/sec

w weight-flow rate, lb/sec

α absolute flow angle measured from axial plane, deg

γ ratio of specific heats

δ ratio of inlet total pressure to NASA standard sea-level pressure, p'_0/p^*

η adiabatic efficiency, ratio of turbine work (based on shaft torque, friction torque, speed, and weight-flow measurements) to ideal work (based on measured inlet total pressure and outlet static pressure)

θ_{cr} squared ratio of critical velocity at turbine inlet to critical velocity at NASA standard sea-level temperature, $(V_{cr,0}/V^*_{cr})^2$

λ speed-work parameter, $U_m^2/(gJ\,\Delta h')$

Subscripts:

a annulus

b reference or base values

cr conditions at Mach number = 1.00

i inlet to blade row

id ideal

le leading edge

m mean radius

max maximum

min minimum

o outlet to blade row

p pressure surface

s suction surface

te trailing edge

u tangential

x	axial
0	station at inlet to turbine (fig. 1)
1	station at throat of first-stage stator
2	station at outlet of first-stage stator just upstream of trailing edge
3	station between first-stage stator and rotor
4	station at inlet to first-stage rotor just downstream of leading edge
5	station at outlet of first-stage rotor just upstream of trailing edge
6	station between first and second stages
7	station at throat of second-stage stator
8	station at outlet of second-stage stator just upstream of trailing edge
9	station between second-stage stator and rotor
10	station at inlet of second-stage rotor just downstream of leading edge
11	station at outlet of second-stage rotor just upstream of trailing edge
12	station downstream of second-stage rotor

Superscripts:

*	NASA standard conditions
'	absolute total state

TURBINE DESIGN

Design Requirements

The design requirements selected for the 4.5-inch-mean-diameter two-stage turbine are as follows:

Over-all equivalent specific work output, $\Delta h'/\theta_{cr}$, Btu/lb	37.2
Over-all speed-work parameter, λ	0.2
Equivalent weight flow, $w\sqrt{\theta_{cr}}/\delta$, lb/sec	0.2
Equivalent horsepower, $hp/\delta\sqrt{\theta_{cr}}$	10.5
Equivalent mean-blade-section velocity, $U_m/\sqrt{\theta_{cr}}$, ft/sec	432

Velocity Diagrams

The design velocity diagrams were constructed at the free-stream stations 0, 3, 6, 9, and 12 for the mean radius to meet the design requirements and are based on the following assumptions and additional specifications:

(1) Two-dimensional flow

(2) Equal work split or speed-work parameter per stage of 0.4

(3) A 1/3 and 2/3 split up of total-pressure loss between the stator and rotor, respectively

(4) Equal rotor-inlet and -outlet relative critical velocity ratio.

A design efficiency was obtained from reference 1 for a stage speed-work parameter of 0.4 and was arbitrarily reduced 5 points to account for anticipated size effects. Thus, the stage design efficiency used in the design was 0.75 (based on total-pressure ratio). Using this stage efficiency results in an over-all design total efficiency for this turbine of 0.775 and an over-all design static efficiency of 0.735. The resulting design over-all total-pressure ratio and design over-all total- to static-pressure ratio are 5.57 and 6.20, respectively.

These free-stream diagrams together with a sketch of the blading showing the station nomenclature used are shown in figure 1. The turning within both stators is comparatively high with exit angles measured from tangential for the first and second stages of 11.76° and 15.87°, respectively. The design turning in the first-stage rotor is 135.02° and that in the second-stage rotor is 119.00°. Further, it can be seen that the first- and second-stage rotors were designed for 21.8° and 13.7° of exit whirl, respectively.

Velocities at stations 2, 4, 5, 8, 10, and 11 for use in the blade design were computed from adjacent free-stream diagrams at stations 3, 6, 9, and 12 and are based on the following assumptions between the adjacent stations:

(1) No change in tangential component of velocity

(2) Continuity and no loss in total pressure.

The blade design velocity diagrams are presented in figure 2 and were computed for 48 stator blades with a trailing-edge thickness of 0.016 inch for each stator blade row and 49 rotor blades with 0.020- and 0.010-inch leading- and trailing-edge thicknesses for each rotor row.

Stator Design

The stator blade profile was laid out to give what was considered to be a smoothly converging channel. No design analysis was made of the blade channel as it was considered unnecessary because of the large acceleration of the flow from inlet to outlet. The first-stage stator was almost choked ($(V/V_{cr})_2 = 0.995$); the first-stage stator mean-radius throat dimension was obtained from the relation ($o_1 = (s_2 - t_2)\cos \alpha_2$). Since the outlet velocity for the second stage was slightly supersonic ($(V/V_{cr})_8 = 1.118$), supersonic expansion downstream of the throat was needed. The second-stage stator mean-radius throat was obtained from the relation $o_7 = (A_{cr}/A)_8(s_8 - t_8)\cos \alpha_8$, where $(A_{cr}/A)_8$ is the critical area ratio corresponding to the supersonic critical velocity ratio $(V/V_{cr})_8 = 1.118$. The blade profile used for the first-stage stator was also used for the second-stage stator. Straight-line suction surfaces were used from the trailing edge to the stator blade throat. The blade mean-radius sections forming the channels for the first- and second-stage stators are shown in figure 3. The stator coordinates are given in table I. The solidity of both stators is 1.78.

In order to obtain design axial velocity in the second stage, it was necessary to increase the annulus area of this stage. This was accomplished by increasing the blade height equal amounts at the hub and tip while maintaining a 4.5-inch mean diameter. The transition from the blade height of the first stage to that of the second stage was accomplished within the second-stage stator by using a sinusoidal variation.

Rotor Design

The rotor blade profiles were laid out for the mean radius and analyzed for continuity and surface velocities by using the method of reference 2 with the exception that radial variations were ignored. The blade profiles forming the first- and second-stage rotor channels are shown in figure 3. The blade surface and midchannel velocity distributions are given in figure 4 for both rotors. The coordinates

for both rotor blades are given in table II. The solidities of the first and second rotors are 1.741 and 1.738, respectively.

Figure 4 shows that the diffusion on the surfaces of the blades is comparatively high. The diffusion parameters on the suction surface D_s of the first and second stage are 0.15 and 0.29, respectively. The diffusion parameters on the pressure surface D_p of the first and second stage are 0.53 and 0.57, respectively.

APPARATUS

The apparatus used in this investigation consisted of the turbine configuration, suitable housing to give uniform turbine-inlet flow conditions, a dynamometer, which was coupled to the rotor through a speed-reducing gear box and a torquemeter shaft, and suitable inlet and outlet piping. A diagrammatic sketch of the turbine test apparatus is shown in figure 5. A cutaway view of the turbine test section showing the measuring stations is shown in figure 6. Dry pressurized air from the laboratory combustion air supply was piped to the turbine-inlet collector (fig. 6) through a sharp-edged orifice run, a pressure regulating valve, air filters, and six rubber hoses. The air leaving the turbine was exhausted through throttle valves to the laboratory altitude exhaust system.

The stator blades were ground from SAE 4340 steel bar stock and were located in the stator rings with slots which were machined through both rings. Each rotor had blades which were machined as integral parts of the rotor disk from aluminum alloy. A rotor tip clearance of 0.012 inch was used for both rotors. An axial clearance of 0.015 inch between the stator and rotor was used. A labyrinth shaft seal was located between the first and second stage to minimize leakage between the two stages.

INSTRUMENTATION

Instrumentation was provided on the turbine apparatus to obtain over-all turbine performance and interstage static-pressure measurements at various speeds and pressure ratios.

Air weight-flow measurements were made with a sharp-edged orifice which was installed in accordance with ASME Power Test Codes. The torque output of the rotor was measured by a strain-gage torquemeter. The strain-gage torquemeter was similar to that described in reference 3 with the exception that it was scaled down such that the test section was 3/4 inch in diameter and the wall thickness was 0.005 inch. Turbine speed was measured by an electronic tachometer in conjunction with a magnetic pickup and a ten-tooth sprocket gear mounted on the rotor shaft.

Turbine-inlet measurements were taken in the annulus upstream of the stator inlet. Two static-pressure taps were installed on the outer wall approximately 180° apart and about one chord length upstream of the stator inlet. A bare-wire thermocouple was used in the flared portion of the collector to minimize effects of Mach number on the reading.

Two stator-outlet static-pressure taps approximately 180° apart for each stage were centrally located in the projected stator flow passage on the outer wall. Rotor-outlet static pressures for each stage were measured with two static taps placed 180° apart on the outer wall. All pressures except the pressure drop across the orifice were measured with mercury manometers. The pressure drop across the orifice was measured with a water manometer.

EXPERIMENTAL PROCEDURE

The experimental investigation was conducted by operating the turbine over a range of inlet total pressures from 24 to 40 inches of mercury absolute and with an inlet temperature of about 80° F. Turbine speed was varied from 80 to 120 percent of design speed (approx. 22,000 rpm) in increments of 2000 rpm. The outlet pressure was varied to give a total- to static-pressure ratio variation of from 4 to 14. Friction torque of the bearings and seals was obtained by motoring the shaft at various speeds and measuring the torque with a strain-gage torquemeter.

CALCULATIONS

The turbine was rated on the basis of the ratio of inlet total pressure to second-stage rotor-discharge static pressure. The inlet total pressure was calculated from weight flow, inlet static pressure, and inlet total temperature from the following equation, which is from reference 4:

$$\frac{w\sqrt{T'}}{pA_a} = \left[\frac{2\gamma g}{(\gamma - 1)R}\right]^{1/2} \left\{\left[\left(\frac{p'}{p}\right)^{\frac{\gamma-1}{\gamma}} - 1\right] + \left[\left(\frac{p'}{p}\right)^{\frac{\gamma-1}{\gamma}} - 1\right]^2\right\}^{1/2}$$

Turbine power was based on the sum of shaft and friction torque and rotor speed. Turbine efficiency was calculated as the ratio of actual turbine power to ideal power based on weight flow, inlet temperature, and over-all total- to static-pressure ratio.

RESULTS AND DISCUSSION

The performance of the subject two-stage turbine is presented in figure 7. In this figure equivalent specific work output $\Delta h'/\theta_{cr}$ and adiabatic efficiency η (based on total- to static-pressure ratio) are plotted against total- to static-pressure ratio p'_0/p_{12}. The efficiency curve shown was computed from the faired work output curve.

Figure 7 shows that, at design equivalent speed, design equivalent work output was obtained at an efficiency of 0.639 compared with 0.735 assumed in the design. At design pressure ratio the equivalent specific work output was 33.2 Btu/lb and the efficiency was 0.656. The choking equivalent weight flow was within 1 percent of the design value of 0.2 pound per second.

From a study of static pressure through the turbine it can be determined if design static-pressure distribution was obtained. Figure 8 presents a comparison between the design and experimentally obtained static pressures at stations 0, 3, 6, 9, and 12 at design over-all pressure ratio and design speed. Shown also is the static-pressure distribution at an over-all pressure ratio of 9 where design work was obtained. The static pressure at each station is given as a ratio to the inlet total pressure. Figure 8 shows close agreement between the experimentally obtained points and the design distribution at an over-all pressure ratio corresponding to the design value. Since design static-pressure distribution was obtained and since design work was not obtained at this pressure ratio, it is evident that the increased losses have considerably reduced the velocity and thus the whirl at the inlet and outlet of the rotor of each stage from that of design. Thus, in order to get design work from this turbine, it was necessary to increase the exit whirl of the second stage by reducing the back pressure.

The variation in torque with speed at design pressure ratio is of interest from the viewpoint of acceleration. Therefore, figure 9 presents the variation in torque (as a ratio to torque at design speed) with speed at approximately design pressure ratio. It can be seen that the torque at zero speed is about twice that at design speed. This variation is typical of a two-stage turbine designed to operate at an over-all speed-work parameter of around 0.25.

ANALYSIS OF RESULTS

Reference 5 presents a method of predicting the efficiency of a turbine from the design velocity diagrams. This method depends on a loss coefficient which must be obtained experimentally. Some of the factors that affect this loss coefficient are blade Reynolds number, blade

surface velocity diffusion, tip clearance, and trailing-edge blockage. By using the loss coefficient of the example turbine of reference 5, it was found that the efficiency predicted for the subject turbine was considerably higher than that experimentally obtained herein. In equation (12) of reference 6 it was shown that blade loss under turbulent-flow conditions varies inversely with Reynolds number based on blade height raised to the 1/5 power. In order to determine if Reynolds number could have an important effect on the difference between the efficiency predicted and that found experimentally, the Reynolds number for the example turbine of reference 5 and for the subject turbine was computed based on a mean of the average static conditions and relative velocities at the inlet and outlet of the rotor and stator. It was found that the Reynolds numbers for the example turbine and the first and second stages of the subject turbine were 550,000, 49,330, and 47,190, respectively. Thus, the Reynolds number ratio would be about 11.5 to 1. Thus, by using the inverse 1/5 power law for turbulent flows, a change in Reynolds number from 550,000 to 49,000 would result in an increase in loss by a factor of 1.63.

The effect of Reynolds number on the over-all efficiency of the subject turbine will be determined in the following manner. In reference 5 the loss in kinetic energy L was related to an average actual kinetic-energy level E_{act} and is given herein by the following relation:

$$L = CE_{act}$$

where C is a loss coefficient defined by different nomenclature in reference 5 as a ratio of loss to average actual kinetic-energy level. It will be assumed that the loss coefficient C varies inversely with Reynolds number to the 1/5 power. Combining the effect of angle variation as indicated in reference 5 and the effect of Reynolds number variation gives the following relation:

$$C = C_b \left(\frac{\cot \alpha_b}{\cot \alpha}\right)\left(\frac{Re_b}{Re}\right)^{1/5}$$

From this equation the new loss coefficients computed for the first and second stages were 0.0912 and 0.0674, respectively. By using these loss coefficients and equations (19), (22), and (26) of reference 5, a variation of over-all efficiency with speed-work parameter was obtained and is presented in figure 10. Shown also in figure 10 is the theoretical efficiency variation of the subject turbine if both stages were operated at a Reynolds number of 550,000. It should be noted that this method neglects reheat and that Reynolds number basically affects the loss in terms of ideal kinetic energy instead of actual kinetic-energy level as was used herein. These effects tend to counterbalance each other since reheat tends to raise the over-all efficiency while the effect of Reynolds number applied to loss in terms of ideal kinetic energy would tend to

reduce it. The difference in level of these curves would tend to give an approximation of the effect of Reynolds number on turbine efficiency.

A comparison of the level of the two curves in figure 10 indicates a higher level of theoretical efficiency for operation at the higher Reynolds number. Further, it is seen that at a speed-work parameter of 0.2 the theoretical over-all efficiency for operation at the higher Reynolds number is 0.744 while for operation at the lower Reynolds number the theoretical over-all efficiency is 0.664. Thus, there is an eight-point reduction in efficiency due to a reduction in Reynolds number by a factor of approximately 11.5.

The experimental points shown in figure 7 are plotted in figure 11 in terms of speed-work parameter together with a segment of the lower Reynolds number curve presented in the previous figure. From figure 11 it can be seen that a mean curve through the experimental points would fall about two efficiency points below the theoretical curve. Since this turbine was designed for relatively high diffusion on the blade surfaces, relatively large tip clearances, and relatively thick leading and trailing edges, the over-all efficiency obtained is expected to be lower than that which could be obtained if the design were aerodynamically optimized.

By using the solid curve in figure 10 the theoretical variation of torque with speed was computed by the method of reference 7 and is plotted in figure 12. In this figure torque is represented by $\Delta V_u/\sqrt{gJ\ \Delta h'_{id}}$ and speed is represented by $U/\sqrt{gJ\ \Delta h'_{id}}$. The experimental points obtained herein were plotted in this figure, and it can be seen that the experimental points fall slightly below the theoretical curve. The close agreement between theoretical and experimental values over the range investigated further indicates the validity of the Reynolds number effect used herein for predicting over-all turbine losses.

SUMMARY OF RESULTS

The results of the investigation of a 4.5-inch-mean-diameter two-stage turbine can be summarized as follows:

1. At design equivalent speed, design equivalent specific work was obtained at a total-to-static efficiency of 0.639.

2. At design pressure ratio, design pressure distribution was obtained with an equivalent specific work output of 33.2 with an efficiency of 0.656.

3. Comparison with theoretical efficiencies based on a loss coefficient and the velocity diagrams were presented to indicate the effect of Reynolds number on turbine efficiency. Close agreement was obtained between theoretical and experimental efficiencies when the loss coefficient was adjusted for changes in Reynolds number to the -1/5 power.

Lewis Research Center
National Aeronautics and Space Administration
Cleveland, Ohio, January 7, 1959

REFERENCES

1. Stewart, Warner L.: Analytical Investigation of Single-Stage-Turbine Efficiency Characteristics in Terms of Work and Speed Requirements. NACA RM E56G31, 1956.

2. Whitney, Warren J., Monroe, Daniel E., and Wong, Robert Y.: Investigation of Transonic Turbine Designed for Zero Diffusion of Suction-Surface Velocity. NACA RM E54F23, 1954.

3. Rebeske, John J., Jr.: Investigation of NACA High-Speed Strain-Gage Torquemeter. NACA TN 2003, 1950.

4. Stewart, Warner L., Wong, Robert Y., and Evans, David G.: Design and Experimental Investigation of a Transonic Turbine with Slight Negative Reaction Across Rotor Hub. NACA RM E53L29a, 1954.

5. Stewart, Warner L.: Analytical Investigation of Multistage-Turbine Efficiency Characteristics in Terms of Work and Speed Requirements. NACA RM E57K22b, 1958.

6. Miser, James W., Stewart, Warner L., and Whitney, Warren J.: Analysis of Turbomachine Viscous Losses Affected by Changes in Blade Geometry. NACA RM E56F21, 1956.

7. Stewart, Warner L.: Torque-Speed Characteristics for High-Specific-Work Turbines. NACA TN 4379, 1958.

TABLE I. - STATOR BLADE COORDINATES

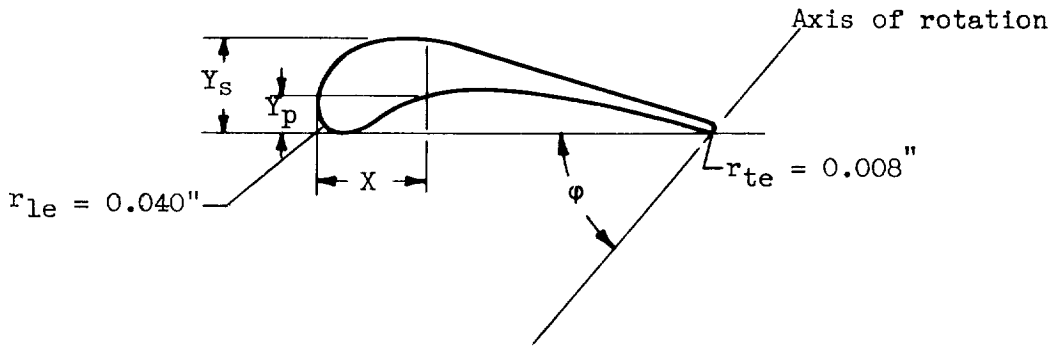

X, in.	Y_p, in.	Y_s, in.
0	0.040	0.040
.050	.001	.112
.100	.026	.129
.150	.044	.128
.200	.054	.115
.250	.056	.100
.300	.051	.085
.350	.042	.070
.400	.030	.054
.450	.018	.038
.500	.004	.023
.523	.008	.008

Stage number	φ
1	57°39'
2	53°23'

TABLE II. - ROTOR BLADE-MEAN-SECTION COORDINATES

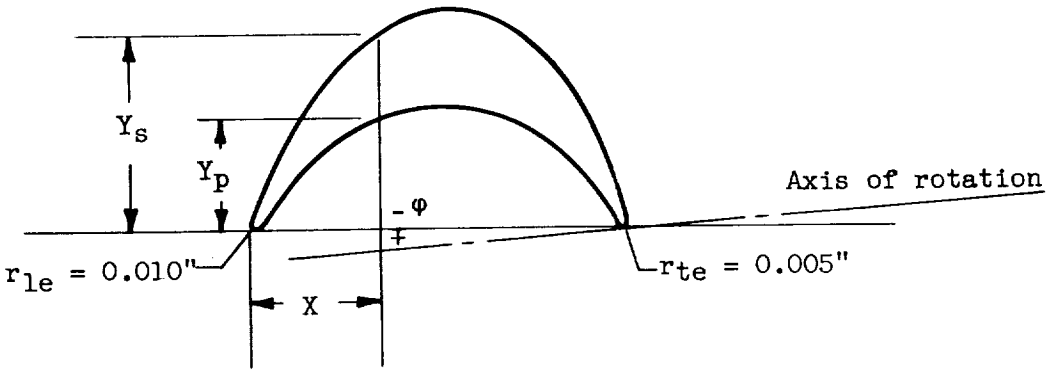

First stage		
φ	$3^{o}45'$	
X, in.	Y_p, in.	Y_s, in.
0	0.010	0.010
.05	.065	.144
.10	.125	.271
.15	.161	.324
.20	.176	.341
.25	.180	.335
.30	.172	.310
.35	.153	.260
.40	.117	.178
.45	.065	.093
.5024	.005	.005

Second stage		
φ	$-0^{o}30'$	
X, in.	Y_p, in.	Y_s, in.
0	0.010	0.010
.05	.051	.098
.10	.100	.179
.15	.133	.255
.20	.151	.286
.25	.158	.289
.30	.152	.267
.35	.135	.219
.40	.103	.150
.45	.054	.080
.5014	.005	.005

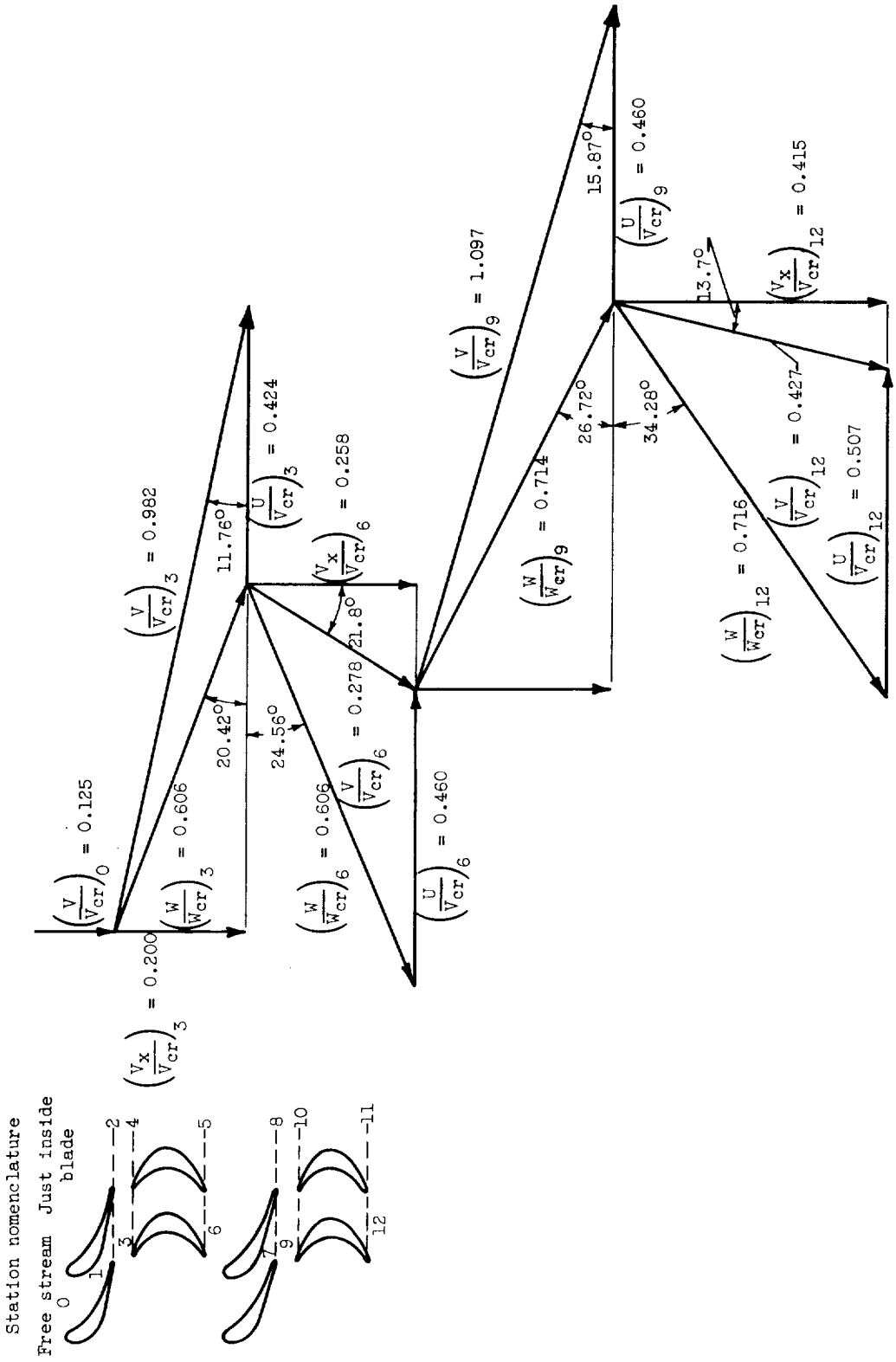

Figure 1. - Free-stream velocity diagrams for 4.5-inch two-stage turbine.

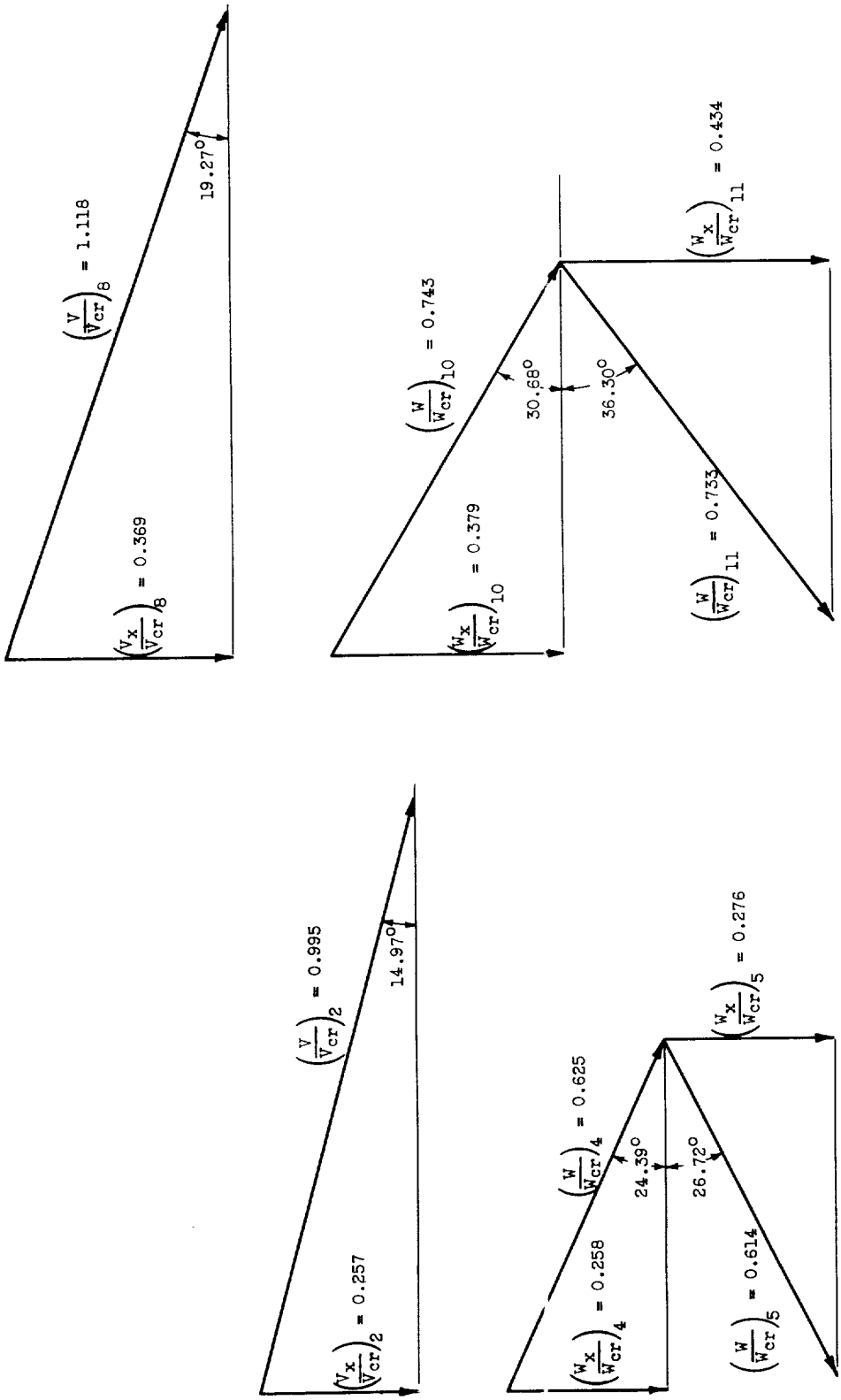

Figure 2. - Blade design velocity diagrams for 4.5-inch two-stage turbine. (See fig. 1 for station nomenclature.)

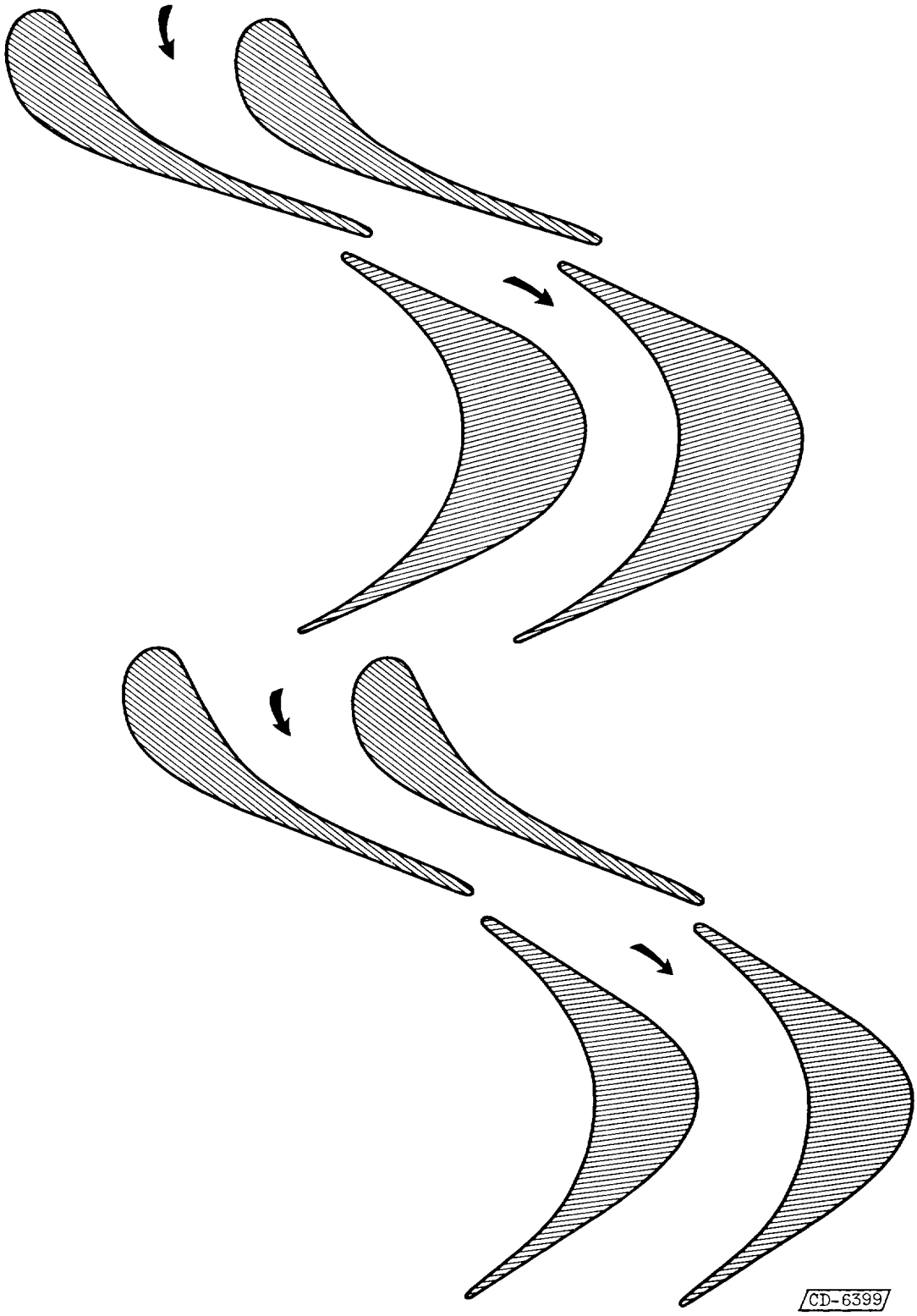

Figure 3. - Stator and rotor blade profiles.

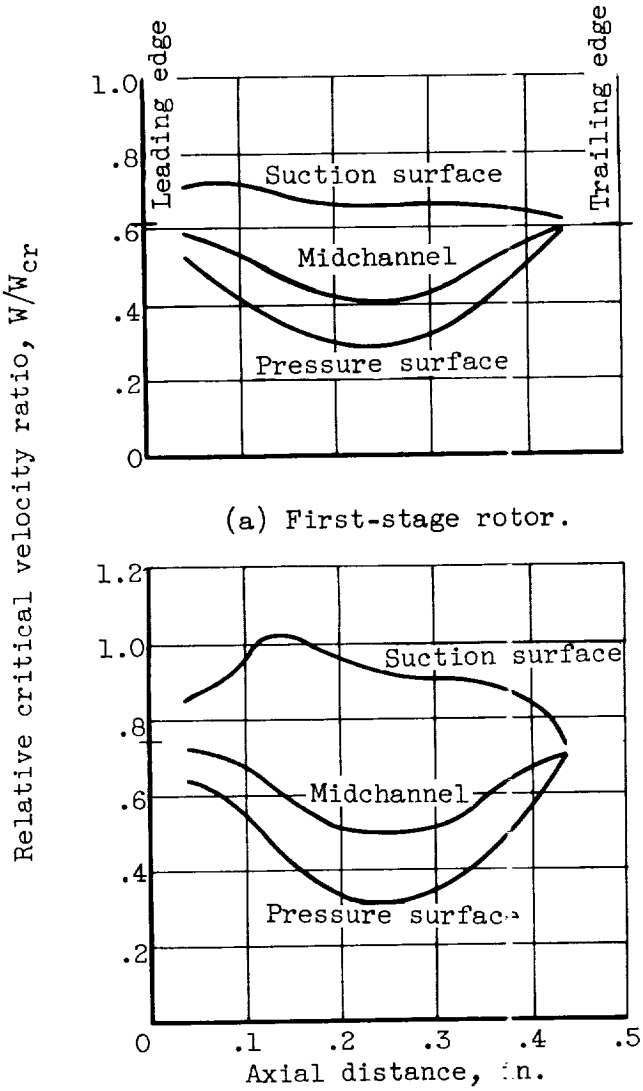

(a) First-stage rotor.

(b) Second-stage rotor.

Figure 4. - Design rotor velocity distributions.

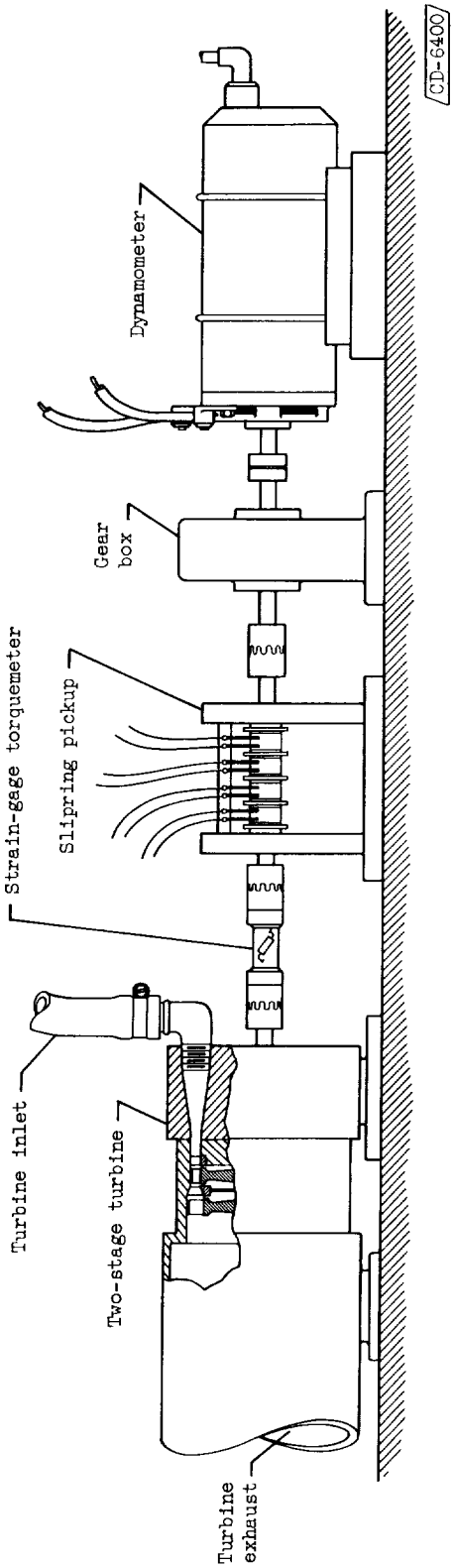

Figure 5. - Test apparatus.

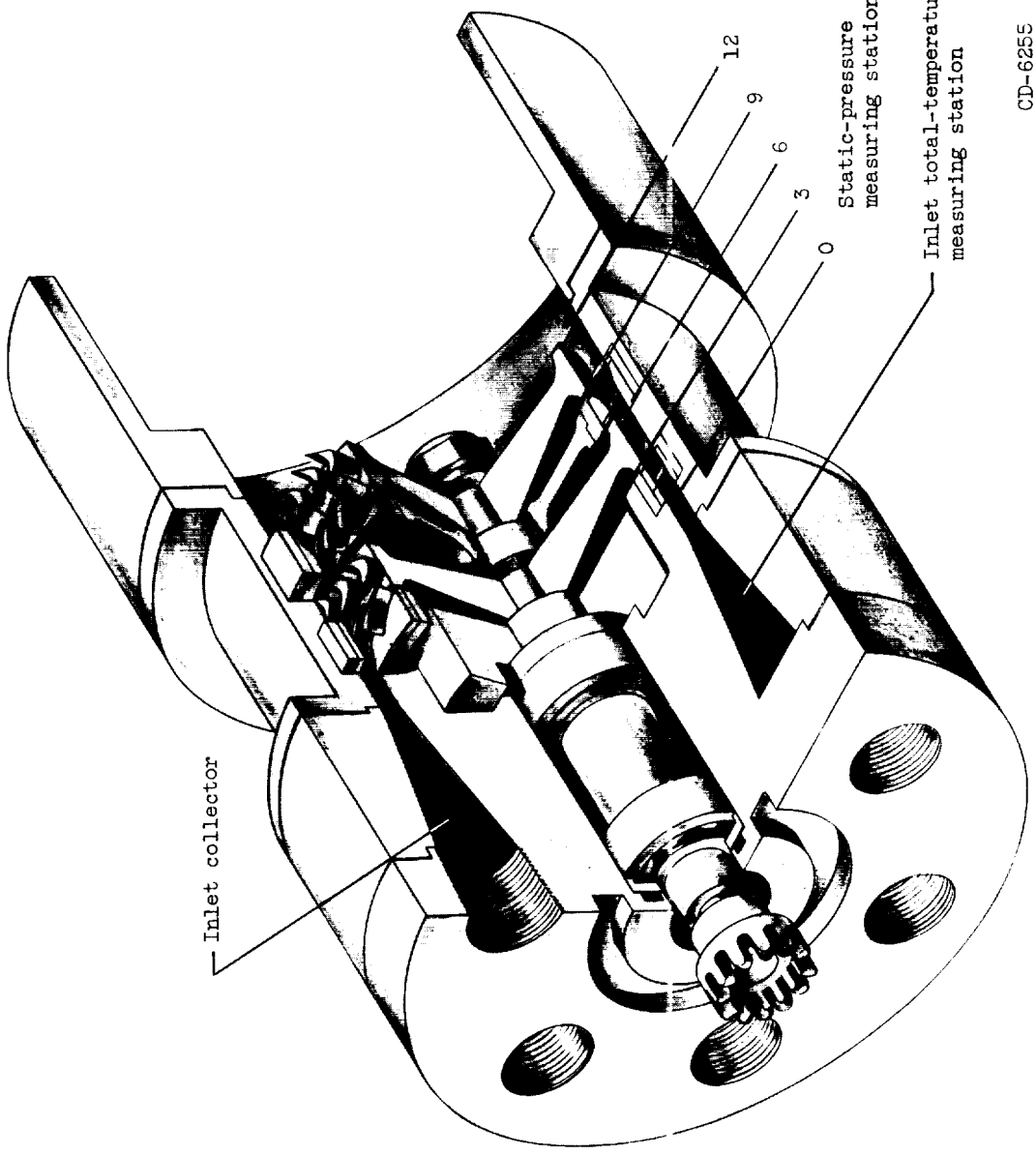

Figure 6. - Cutaway view of 4.5-inch two-stage turbine.

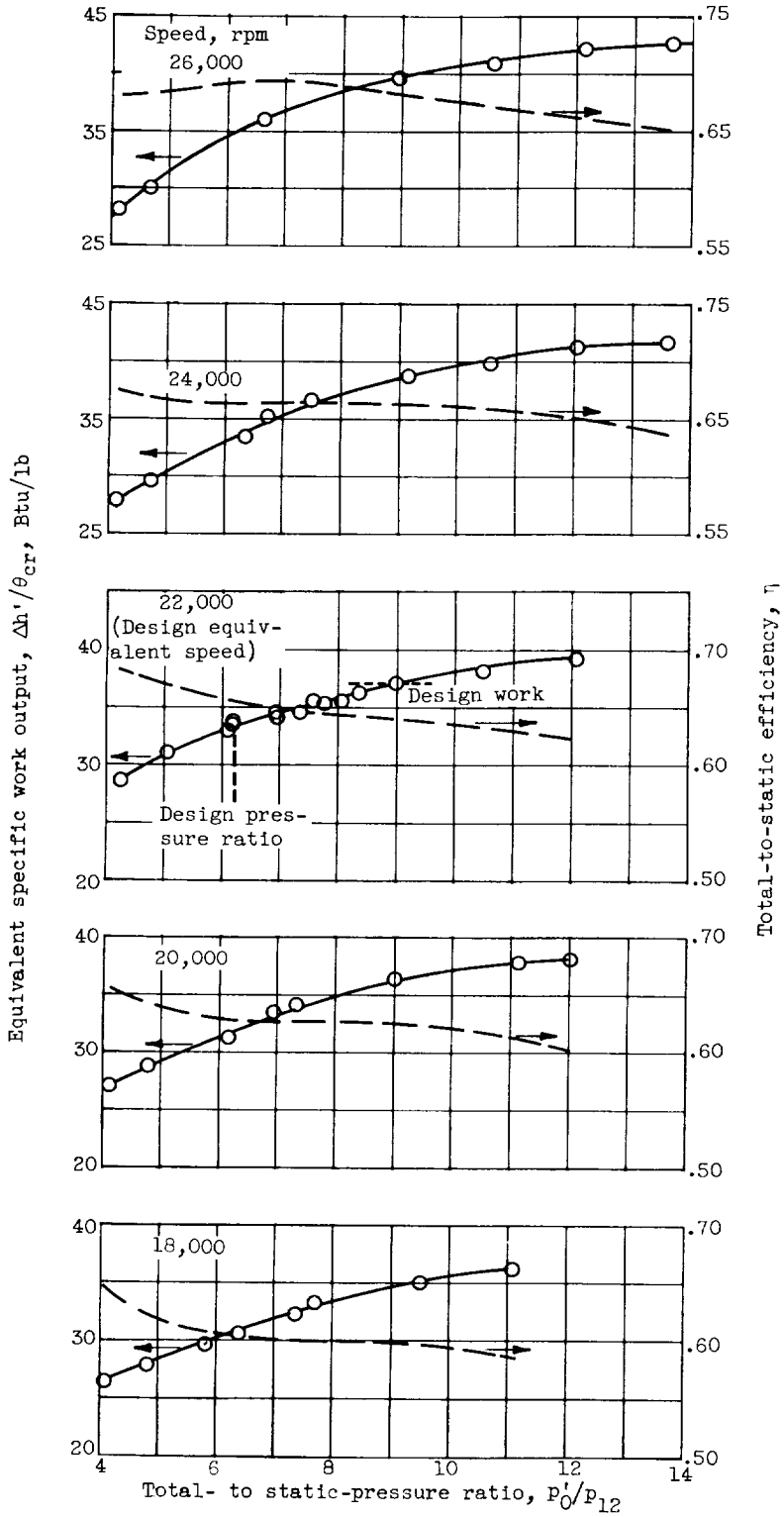

Figure 7. - Experimentally obtained performance of 4.5-inch-mean-diameter two-stage turbine.

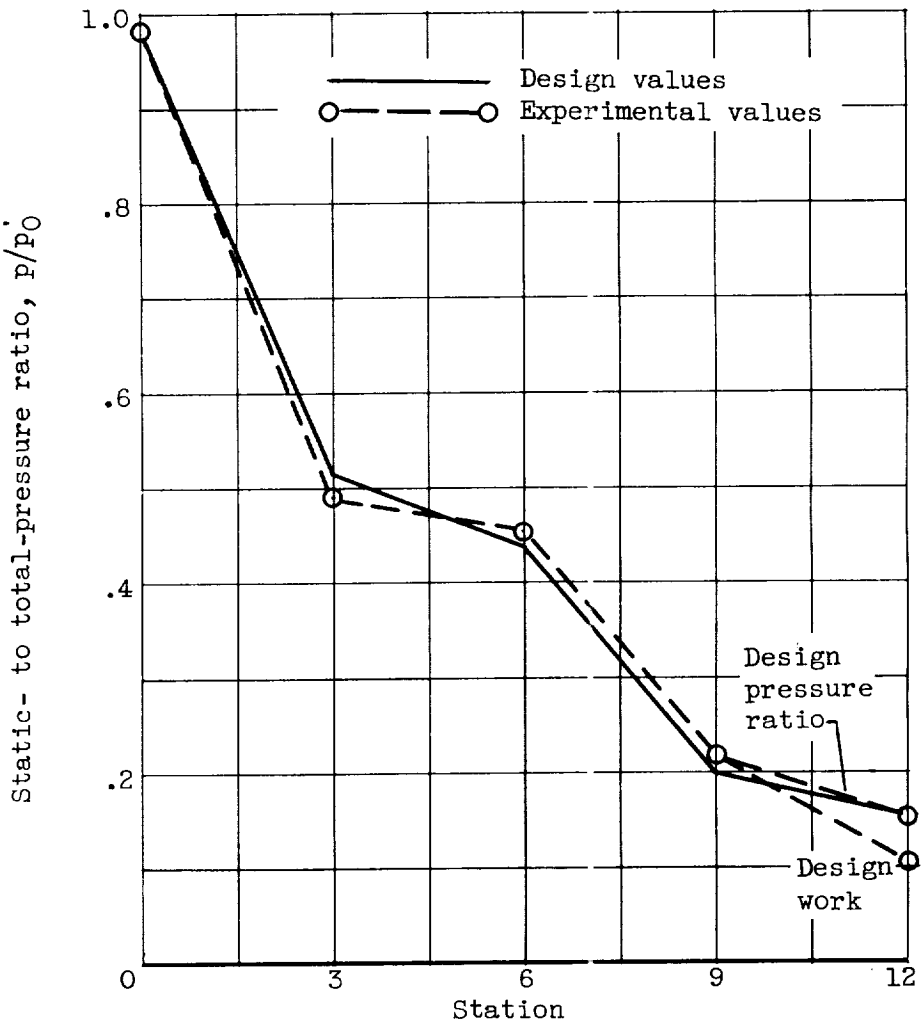

Figure 8. - Comparison of design and experimental static-pressure variation through turbine.

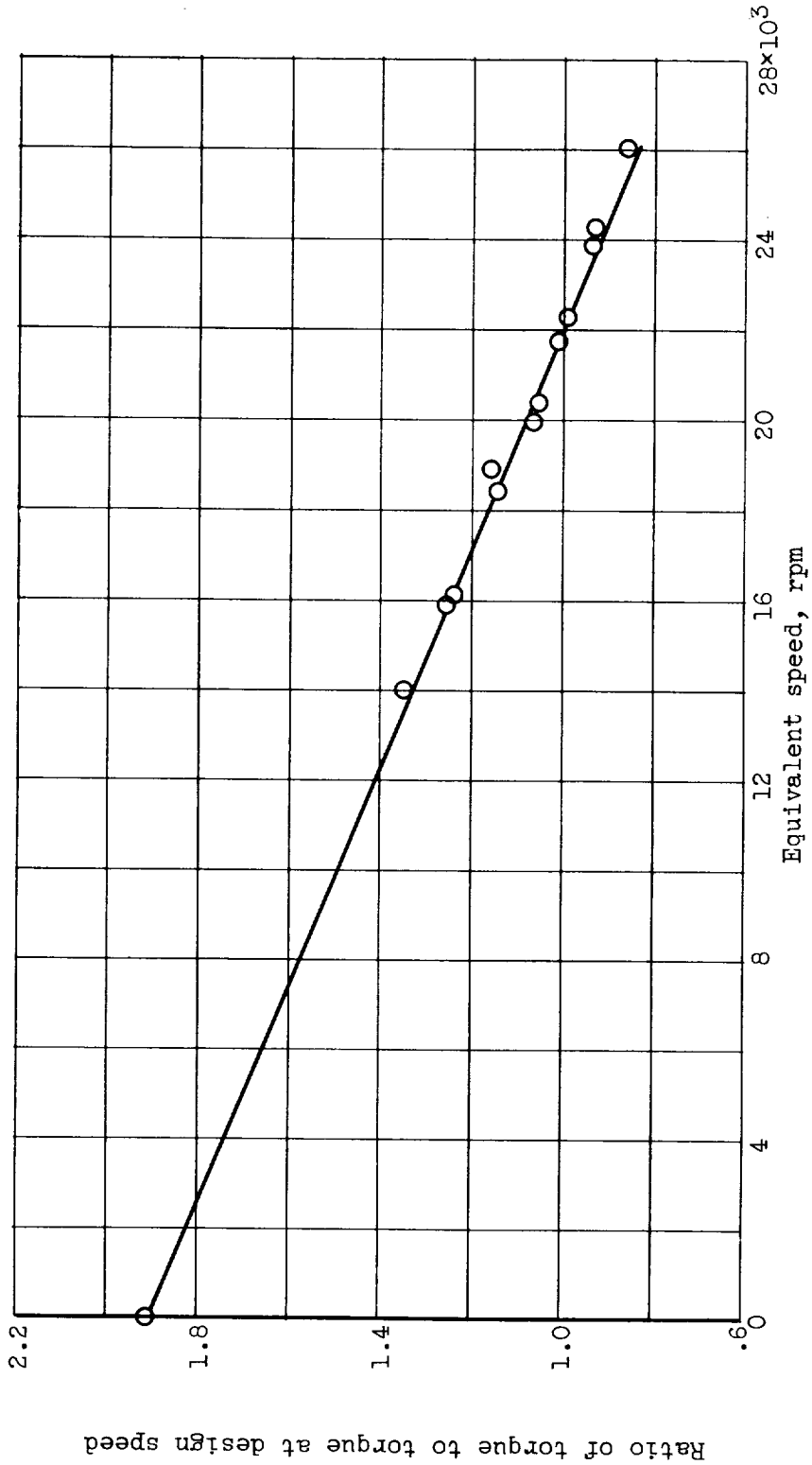

Figure 9. - Experimental variation of torque with speed at approximately design pressure ratio.

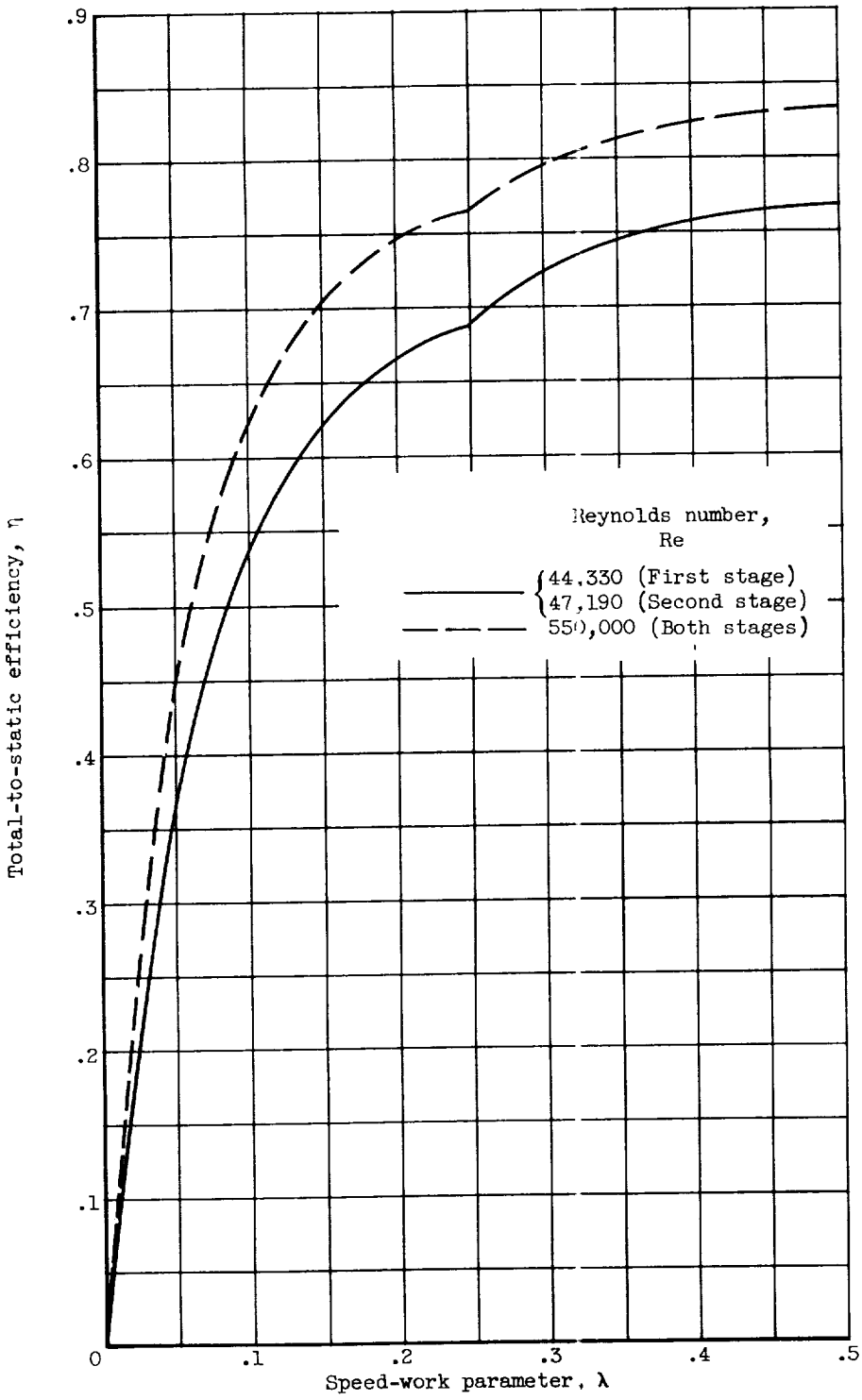

Figure 10. - Over-all static efficiency characteristics for two-stage turbine. First-stage flow angle α_3, 78.24°; second-stage flow angle α_9, 74.13°.

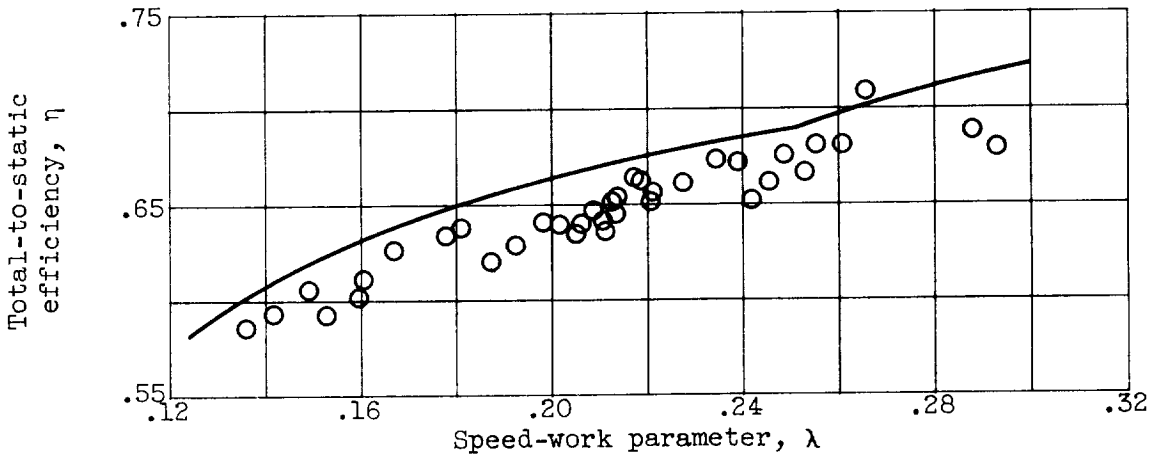

Figure 11. - Comparison of theoretical variation of efficiency with speed-work parameter with experimental variation.

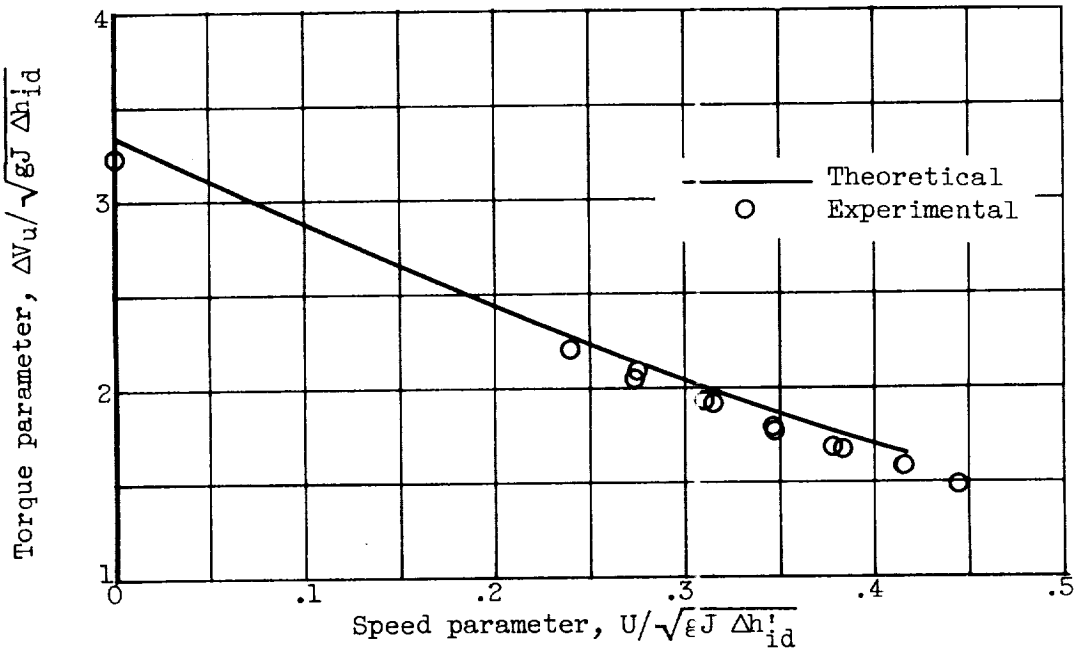

Figure 12. - Comparison of theoretical and experimental variation of torque with speed.